Inorg. Chem. **2003**, *42*, 3067–3073

Tetrakis(imidazolyl)borate-Based Coordination Polymers: Group II Network Solids, $M[B(Im)_4]_2(H_2O)_2$ (M = Mg, Ca, Sr)

Barton H. Hamilton, Kathryn A. Kelly, Wilhelm Malasi, and Christopher J. Ziegler*

Department of Chemistry, University of Akron, Akron, Ohio 44325-3601

Received December 6, 2002

We are using the coordinating anion tetrakis(imidazolyl)borate to construct new metal–organic framework structures. In this report, we present three alkaline earth metal network solids incorporating this anion. All three compounds have the same formula, $M[B(Im)_4]_2(H_2O)_2$ (M = Mg, Ca, Sr), and the same coordination environment about the metal. However, the three compounds have different network structures with different degrees of hydrogen bonding; the Mg material forms a two-dimensional network and the Ca and Sr compounds form one-dimensional chains. In addition, we present the structure of the protonated anion $B(HIm)(Im)_3$ as a model for the default structure of this anion and discuss how the conformation of tetrakis(imidazolyl)borate can affect the structure of network solids.

Introduction

The construction of metal−organic frameworks is an area of continued interest that has developed into a mature field over the past decade.[1] Much of the current study into coordination polymer based crystal design is focusing on two areas: the generation of solids with desired physical or chemical properties[2] and the control of the topology of a particular solid or family of materials.[3] With regard to the latter problem, molecular components based on pyridine (such as 4,4′-bipyridine) or carboxylic acids (such as 1,3,5-benzene tricarboxylate or 1,3,5,7-adamantane tetracarboxylate) have been and continue to be extensively examined.[4] Researchers can explore the parameter spaces of design methodology and resultant structure through factors such as the ratio of components, the type of metal center, or the inclusion of templating reagents. Zaworotko and Yaghi both provide good descriptions of the recent developments in this rapidly evolving field.[1,5]

In our work, we have chosen to examine tetrakis(imidazolyl)borate, $B(Im)_4^-$, as an organic component of network solids. Tetrakis(azolyl)borates were first generated in 1967, but have not been previously investigated as a component of metal−organic frameworks.[6] Tris(azolyl)borates, including tris(imidazolyl)borates, have been examined as components for network systems, however.[7] Using boron as a scaffold affords several advantages to the organic fragment in network solids.[8] First, borate anions are inherently tetrahedral and thus can promote the formation of three-dimensional solids. In addition, the anionic character of this organic component can balance the charge of the metals in the solid. This can eliminate the need for noncoordinating anions in the network matrix. Finally, tetrakis(imidazolyl)borate is easy to synthesize from cheap and commercially available reagents, and functionalized variants can be readily generated. We have recently reported on this coordinating anion in the synthesis of a functional network solid, $Pb[B(Im)_4])(NO_3)(1.35H_2O)$.[9] However, in addition to syn-

* Author to whom correspondence should be addressed. E-mail: ziegler@uakron.edu.

(1) (a) Barton, T. J.; Bull, L. M.; Klemperer, W. G.; Loy, D. A.; McEnaney, B.; Misono, M.; Monson, P. A.; Pez, G.; Scherer, G. W.; Vartuli, J. C.; Yaghi, O. M. *Chem. Mater.* **1999**, *11*, 2633−2656. (b) Blake, A. J.; Champness, N. R.; Hubberstey, P.; Li, W. S.; Withersby, M. A.; Schroder, M. *Coord. Chem. Rev.* **1999**, *183*, 117−138. (c) Eddaoudi, M.; Moler, D. B.; Li, H. L.; Chen, B. L.; Reineke, T. M.; O'Keeffe, M.; Yaghi, O. M. *Acc. Chem. Res.* **2001**, *34*, 319−330. (d) Zaworotko, M. J. *Nature* **1999**, *402*, 242−243. (e) Yaghi, O. M.; Li, H. L.; Davis, C.; Richardson, D.; Groy, T. L. *Acc. Chem. Res.* **1998**, *31*, 474−484.

(2) Evans, O. R.; Lin, W. B. *Acc. Chem. Res.* **2002**, *35*, 511−522.

(3) Zaworotko, M. J. *Chem. Soc. Rev.* **1994**, *23*, 283−288.

(4) (a) Yaghi, O. M.; Davis, C. E.; Li, G. M.; Li, H. L. *J. Am. Chem. Soc.* **1997**, *119*, 2861−2868. (b) Fletcher, A. J.; Cussen, E. J.; Prior, T. J.; Rosseinsky, M. J.; Kepert, C. J.; Thomas, K. M. *J. Am. Chem. Soc.* **2001**, *123*, 10001−10011. (c) Chen, B. L.; Eddaoudi, M.; Reineke, T. M.; Kampf, J. W.; O'Keeffe, M.; Yaghi, O. M. *J. Am. Chem. Soc.* **2000**, *122*, 11559−11560. (d) Noro, S.; Kitaura, R.; Kondo, M.; Kitagawa, S.; Ishii, T.; Matsuzaka, H.; Yamashita, M. *J. Am. Chem. Soc.* **2002**, *124*, 2568−2583.

(5) Moulton, B.; Zaworotko, M. J. *Chem. Rev.* **2001**, *101*, 1629−1658.

(6) (a) Trofimenko, S. *J. Am. Chem. Soc.* **1967**, *89*, 3170−3177. (b) Trofimenko, S. *J. Coord. Chem.* **1972**, *2*, 75−77.

(7) (a) Janiak, C.; Scharmann, T. G.; Albrecht, P.; Marlow, F.; Macdonald, R. *J. Am. Chem. Soc.* **1996**, *118*, 6307−6308. (b) Janiak, C.; Temizdemir, S.; Dechert, S. *Inorg. Chem. Commun.* **2000**, *3*, 271−275.

(8) Greenwood, N. N. *Boron*; Pergamon Press: Oxford, 1975.

10.1021/ic026244x CCC: $25.00
Published on Web 04/10/2003

thesizing functional solids, we also wish to understand how this anion forms extended network structures, such as with simple divalent metal cations.

In this paper, we report the synthesis and structures of three group II metal cation networks incorporating $B(Im)_4^-$. All three compounds have the empirical formula $M[B(Im)_4](H_2O)_2$ where M = Mg, Ca, and Sr. These three network solids have the same ligand set coordinated about the metal center, including four imidazole rings and two axial water molecules. However, by changing the metal cation, the morphology of the structure alters significantly between the three compounds. Altered factors include the geometry about the metal center, the conformation of the borate, and the extent of hydrogen bonding in the solid. In addition, we have investigated the structure of the protonated form of the borate anion, the neutral species $B(HIm)(Im)_3$. We can use this "anion-only" structure to examine conformational minima of tetrakis(imidazolyl)borate, and compare the preferred conformation to the borate conformations observed in the three metal network solids.

Experimental Section

All reagents and solvents were purchased from Aldrich and used as received. Water was purified by using a Milli-Q reagent water system. Mass spectra were obtained on a Micromass AutoSpec EBEhQ hybrid tandem mass spectrometer using FAB ionization. Solution NMR spectroscopy was performed on a Varian VXR 300 MHz NMR instrument. Elemental analysis was carried out at the School of Chemical Sciences Microanalytical Laboratory at the University of Illinois at Urbana−Champaign. Nitrogen analyses tend to be lower than calculated due to the formation of refractory boron nitrides.[10] Thermogravimetric analysis was measured on a TA Instruments 2050 device. Solid-state NMR spectra were obtained on a Varian Unityplus-200 (4.7 T) spectrometer using Doty Scientific supersonic and standard MAS probes.

Synthesis of $Na[B(Im)_4]$. The synthesis of this material was based on a procedure developed by Trofimenko for sodium tetrakis(pyrazolyl)borate and is described by Chao and co-workers.[6,11] In a nitrogen-flushed flask attached to an oil bubbler, sodium borohydride (3.78 g, 0.1 mol) and imidazole (54.5 g, 0.8 mol) were mixed and heated to a temperature of 225 °C. The evolution of hydrogen gas from the reaction flask was monitored, and the reaction proceeded for 1.5 h, after which the evolution of gas ceased. The reaction flask was cooled to room temperature, and acetone (100 mL) was added to the reaction mixture. The acetone dissolves the unreacted imidazole and reaction byproducts, leaving the product $Na[B(Im)_4]$ as an off-white solid. The crude product was then recrystallized from ethanol, affording 27.8 g of product (92% yield). ^{1}H NMR (D_2O): 6.856 (H-5), 7.055 (H-4), 7.233 (H-2) ppm. ^{13}C NMR: 122.28, 128.50, 140.92 ppm. ^{11}B NMR (D_2O) 2.117 ppm. FAB MS (negative ion): 279 *m*/*z* ($B(Im)_4^-$). IR (KBr): 3145, 3125, 3113, 3039, 2917, 2824, 2613, 2536, 2498, 2437, 1696, 1614, 1475, 1293, 1247, 1208, 1109, 1082, 1040, 923, 819, 776 cm^{-1}.

Synthesis of $B(HIm)(Im)_3$ (1). $Na[B(Im)_4]$ (250 mg, 0.8 mmol) was dissolved in 25 mL of H_2O at room temperature in a flask. To this solution was added 825 μL of 1.0 M HCl with stirring, and the pH of the resultant mixture approached neutrality. At this point, 100 μL aliquots of 1.0 M HCl were added to the solution until a while precipitate formed and the pH decreased to 6.9. The precipitate was collected by filtration and dried, affording 173 mg of product (69% yield). ^{1}H NMR (D_2O): 7.026 (H-5), 7.238 (H-4), 7.530 (H-2) ppm. ^{13}C NMR: 122.03, 127.23, 139.43 ppm. ^{11}B NMR (D_2O) 2.327 ppm. FAB MS (negative ion): 279 *m*/*z* ($B(Im)_4^-$). IR (KBr): 3449 3142, 3109, 3084, 3004, 2535, 2024, 1630, 1580, 1523, 1476, 1336, 1287, 1267, 1252, 1220, 1206, 1182, 1112, 1104, 1079, 935, 757, 669 cm^{-1}. CHN anal. Calcd for $C_{12}H_{13}N_8B$: C, 51.42; H, 4.64; N, 40.00. Found: C, 50.23; H, 4.57; N, 37.92.

Synthesis of $M[B(Im)_4]_2(H_2O)_2$ (M = Mg (2), Ca (3), Sr (4)). A 1:1 water:ethanol solution (10 mL) of $Na[B(Im)_4]$ (60 mg, 0.2 mmol) was carefully layered over an aqueous solution (10 mL) of $M(X)_2 \cdot nH_2O$ ($Mg(NO_3)_2$, $Ca(OAc)_2 \cdot H_2O$, $Sr(NO_3)_2$, 0.1 mmol) in a narrow test tube. The tubes were then sealed and placed in an oven and the two layers allowed to diffuse slowly over 1 week at 60 °C, after which product was collected by filtration.

$Mg[B(Im)_4]_2(H_2O)_2$: 57 mg (92%). Solid-state ^{13}C MAS NMR: 122.4, 130.1, 132.0, 138.0, 141.2 ppm. IR (KBr): 3132, 3116, 3099, 2705, 2304, 1681, 1626, 1479, 1299, 1289, 1249, 1214, 1116, 1087, 934, 812, 759, 662 cm^{-1}. CHN anal. Calcd for $C_{24}H_{28}N_{16}B_2O_2Mg$: C, 46.59; H, 4.57; N, 36.23. Found: C, 46.40; H, 4.88; N, 34.66.

$Ca[B(Im)_4]_2(H_2O)_2$: 49 mg (78%). Solid-state ^{13}C MAS NMR: 119.9, 129.9, 140.3 ppm. IR (KBr): 3112, 3098, 2621, 2440, 1704, 1693, 1609, 1472, 1302, 1246, 1208, 1110, 1081, 932, 819, 753, 664 cm^{-1}. CHN anal. Calcd for $C_{24}H_{28}N_{16}B_2O_2Ca$: C, 45.43; H, 4.45; N, 35.33. Found: C, 45.09; H, 4.67; N, 33.80.

$Sr[B(Im)_4]_2(H_2O)_2$: 54 mg (80%). Solid-state ^{13}C MAS NMR: 120.5, 129.7, 140.5 ppm. IR (KBr): 3124, 3108, 3083, 2441, 1701, 1627, 1474, 1301, 1246, 1210, 1110, 1081, 929, 819, 757, 666 cm^{-1}. CHN anal. Calcd for $C_{24}H_{28}N_{16}B_2O_2Sr$: C, 42.27; H, 4.14; N, 32.87. Found: C, 41.88; H, 3.96; N, 30.73.

Thermogravimetric Analysis. The TGA of compounds **2**, **3**, and **4** were carried out over a temperature range of 25−600 °C at a scan rate of 10 °C/min. Water loss (2 water molecules per formula unit) occurred between the temperatures of 172 and 209 °C for compound **2**, 134 and 152 °C for compound **3**, and 115 and 138 °C for compound **4**. Decomposition of the three solids started at 287, 297, and 194 °C for **2**, **3**, and **4** respectively.

X-ray Crystallography. For **1**, X-ray intensity data were measured at 100 K (Bruker KRYO-FLEX) on a Bruker SMART APEX CCD-based X-ray diffractometer system equipped with a Mo-target X-ray tube (λ = 0.71073 Å) operated at 2000 W power. A clear crystal was mounted on a cryoloop using Paratone N-Exxon oil and placed under a stream of nitrogen at 100 K. The detector was placed at a distance of 5.009 cm from the crystal. Analysis of the data showed negligible decay during data collection. The data were corrected for absorption with the SADABS program (ratio of minimum to maximum apparent transmission: 0.690050). Additional experimental details are provided in Table 1. The asymmetric unit for **1** is shown in Figure 1. The structure was refined using the Bruker SHELXTL (version 6.1) software package, in the space group $P2_1$, with $Z = 2$ for the formula unit $BC_{12}H_{13}N_8$. The structure was solved using direct methods until the final anisotropic full-matrix least-squares refinement on F^2 converged.[12]

For compounds **2**, **3**, and **4**, X-ray data were collected using Mo (0.71073 Å) radiation on a Syntex P21 diffractometer. The crystals

(9) Hamilton, B. H.; Kelly, K. A.; Wagler, T. A.; Espe, M. P.; Ziegler, C. J.; *Inorg. Chem.* **2002**, *41*, 4984−4986.
(10) Williams, D.; Pleune, B.; Kouvetakis, J.; Williams, M. D.; Andersen, R. A. *J. Am. Chem. Soc.* **2000**, *122*, 7735−7741.
(11) Chao, S. M.; Carl E. *Anal. Chim. Acta* **1978**, *100*, 457−467.
(12) Sheldrick, G. M. *SHELXTL, Crystallographic Software Package*, version 6.10; Bruker-AXS: Madison, WI, 2000.

Table 1. Crystal Data and Structural Refinement Parameters for **1**−**4**

	1	**2**	**3**	**4**
formula	$BC_{12}H_{13}N_8$	$MgB_2C_{24}H_{28}N_{16}O_2$	$CaB_2C_{24}H_{28}N_{16}O_2$	$SrB_2C_{24}H_{28}N_{16}O_2$
formula weight	280.10	618.55	634.32	681.86
cryst syst	monoclinic	monoclinic	triclinic	triclinic
space group	$P2_1$	$P2_1/c$	$P\bar{1}$	$P\bar{1}$
a, Å	7.101(2)	9.6970(19	9.3893(19)	9.4104(19)
b, Å	9.989(3)	14.113(3)	9.6820(19)	9.809(2)
c, Å	9.209(3)	11.451(2)	10.384(2)	10.525(2)
α, deg	90	90	93.39(3)	94.04(3)
β, deg	93.932(6)	114.54(3)	108.36(3)	107.87(3)
γ, deg	90	90	118.04(3)	117.87(3)
vol, Å^3	651.7(4)	1425.7(5)	766.2(3)	790.5(3)
Z	2	2	1	1
ρ(calc), Mg/m^3	1.428	1.441	1.375	1.432
μ, mm^{-1}	0.095	0.119	0.258	1.756
F(000)	292	644	330	348
reflns collected	3939	2989	3239	3331
indep reflns	2167	2514	2701	2779
GOF on F^2	1.137	1.029	1.053	1.110
R [$I > 2\sigma(I)$]	R1 = 0.0559, wR2 = 0.1502	R1 = 0.0685, wR2 = 0.1066	R1 = 0.0340, wR2 = 0.0655	R1 = 0.0504, wR2 = 0.0971
R (all data)	R1 = 0.0597, wR2 = 0.1522	R1 = 0.1558, wR2 = 0.1334	R1 = 0.0473, wR2 = 0.0702	R1 = 0.0722, wR2 = 0.1111

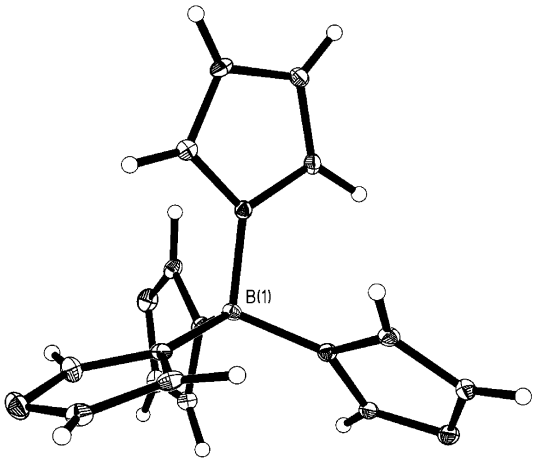

Figure 1. The asymmetric unit of $B(HIm)(Im)_3$.

were coated in Paratone N-Exxon oil, mounted on a glass fiber, and placed under a cold stream of nitrogen at 159 K. Unit cell parameters were obtained by a least-squares analysis of 20 well-centered reflections with $20° < 2\theta < 30°$. The structures were refined using the Bruker SHELXTL (version 6.1) software package and solved using direct methods until the final anisotropic full-matrix least-squares refinement on F^2 converged.[10] Additional experimental details are given in Table 1. The asymmetric units for structures **2**, **3**, and **4** are shown in Figure 2.

Results and Discussion

In order to understand how tetrakis(imidazolyl)borate forms extended networks with metals, we decided to examine the structure and conformations of this organic anion more closely. As can be seen in Figure 1, the central boron atom has a tetrahedral geometry. The bond angles about the central atom are close to the ideal of 109.5°, as determined by inspection of the crystal structure of $B(HIm)(Im)_3$. The measured angles range between 106.1(3)° and 112.0(4)°. The directionality of the coordinating nitrogen, however, deviates from tetrahedral due to the asymmetry of the imidazole ring. In the protonated borate structure, the external nitrogen diverges from the ordinate of the B−N bond by an average of 18.8°, reducing the symmetry of the entire anion.

If the imidazole rings can rotate freely about the B−N bond, then it is clear that a variety of conformations can result. Predicting the low-energy geometries of this anion is a complex problem. Fortunately, the nature of our inquiry is similar to the work carried out by Mislow and co-workers in the 1970s on tetraphenylmethane and its derivatives.[13] As in tetraphenylmethane, the various conformations of tetrakis(imidazolyl)borate can be considered as the imposition of four rotors around the central boron atom. Some of the simpler conformations of $B(Im)_4^-$ are shown in Figure 3.

The highest symmetry conformations of $B(Im)_4^-$ can be designated as open or closed. With a symmetric cyclopentadiene (as shown at the top of the figure), both the open and closed forms would have D_{2d} symmetry. However, the reduced symmetry of the imidazole ring increases the number of open and closed conformations, resulting in a variety of high- and low-symmetry orientations. In addition, if one or more of the B−N bonds rotate from either of these open or closed geometries, a larger number of conformations result. As in tetraphenylmethane, rotation can be defined by an angle φ, the dihedral angle relative to the N−B−N plane. However, a ring can convert from an open to a closed orientation merely by rotating $\pi/6$ rad, or 30°. A variety of lower symmetry orientations can thus be imagined, including C_s, C_2, or C_1. We are currently examining the energy surface for the rotamers of this anion, including both the steric repulsion and bonding interactions that lead to preferred conformations. The steric interactions inhibit the molecule from adopting closed (coplanar) conformations, while the overlap of the π system is maximized by this orientation.

In our crystal structures, we can observe the orientations that the tetrakis(imidazole)borates adopt. Table 2 lists the deviations in degrees from closed orientations for all of the imidazole rings in the four structures presented in this paper. The angles in Table 2 were measured by examining the dihedral angle between the plane of the imidazole ring and the closest B−N bond. A closed conformation will have an

(13) (a) Hutchings, M. G.; Andose, J. D.; Mislow, K. *J. Am. Chem. Soc.* **1975**, *97*, 4553−4561. (b) Hutchings, M. G.; Andose, J. D.; Mislow, K. *J. Am. Chem. Soc.* **1975**, *97*, 4562−4570.

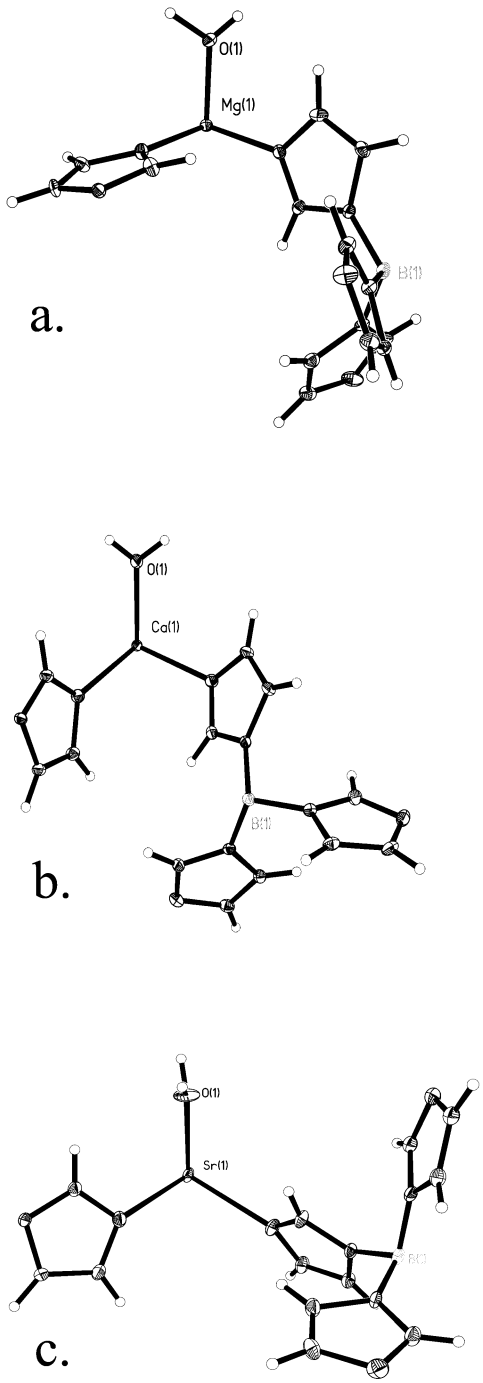

Figure 2. Asymmetric units of $M[B(Im)_4]_2 \cdot 2H_2O$, where M = Mg (a), Ca (b), and Sr (c).

Table 2. Angle Deviations from the Closed Orientation for the Borates in Compounds **1**−**4**

compound	angle deviations from closed (deg)
$B(HIm)(Im)_3$	20.78, 10.53, 16.32, 19.49
$Mg[B(Im)_4]_2(H_2O)_2$	20.73, 33.86, 16.33, 17.39
$Ca[B(Im)_4]_2(H_2O)_2$	30.07, 32.26, 28.65, 35.41
$Sr[B(Im)_4]_2(H_2O)_2$	26.75, 34.59, 34.99, 26.15

angle of 0°, and an open form will have an ideal angle of 30°. In the protonated form of the anion, all of the deviations are in the intermediate region between open and closed, ranging from about 10° to 20°. In the magnesium compound, the angles increase, with one in an open position with an angle measurement of 33.86°. The measured angles can increase above 30° due to the slight deformation of the imidazole ring out of the plane of the B−N bond. In the strontium and calcium materials, all of the rings are in open positions, with angle measurements close to the ideal value of 30°.

We can speculate that this change from intermediate to open angles arises from the increase in π donation from the imidazole ring to metal centers as one goes from Mg to Ca and Sr.[14] The configuration of the protonated form represents an intermediate between the closed geometry, which maximizes π interactions between rings on the borate, and the open geometry, which minimizes steric repulsions. When the imidazole ring binds to a metal center, it can act as both a σ and π base, donating electron density into the metal center. Either π donation or acceptance will disrupt the boron-bridged imidazole-to-imidazole interaction, and decrease the tendency to maximize overlap by forming closed configurations. Without the driving force to form a closed configuration, the steric repulsions dominate the geometry and open positions result. While there are hydrogen-bonding differences between the Mg and Ca and Sr materials, it is important to note that the change from intermediate to open positions has no relationship with hydrogen bonding in the solid; in the Mg structure the hydrogen-bonded imidazole ring has an intermediate geometry (20.73°).

The multiplicity of conformations in tetrakis(imidazolyl)-borate makes it difficult for us to predict how this anion will form extended network solids. However, in the three coordination polymers presented in this paper, the connectivity between the borate and the metal center is much simpler than might be expected. As can be seen in the formula for each of the three compounds, there are two borates and two waters per metal center. Since each metal has an octahedral coordination environment and since both water molecules are coordinating, only two of the imidazole rings per borate are bound to each metal site. Thus, there are only two angle measurements that we need to consider in order to examine the extended network structure of the three metal−organic frameworks presented in this paper: the angle between equatorial positions about the metal (either 90° or 180°) and the metal−borate−metal angle (∼90°).

In all three of the coordination networks with the divalent group II metal cations, the geometry about the metal center is identical (Figure 4). Table 3 lists selected bond distances and angles for the three metal compounds. Each metal center in the three solids is in an octahedral coordination environment, with four imidazole rings in the equatorial positions, and two solvent water molecules in the axial positions. As expected, the metal−ligand bond distances lengthen as one goes down the period. The metal−nitrogen bond distance increases from an average of 2.191(3) Å in $Mg[B(Im)_4]_2(H_2O)_2$ to 2.4752(18) Å in $Ca[B(Im)_4]_2(H_2O)_2$ and 2.638(4) Å in $Sr[B(Im)_4]_2(H_2O)_2$. Similarly, the metal−oxygen bond

(14) (a) Harder, S. *Organometallics* **2002**, *21*, 3782−3787. (b) Bonomo, L.; Solari, E.; Scopelliti, R.; Floriani, C. *Chem. Eur. J.* **2001**, *7*, 1322−1332. (c) Fleischer, R.; Stalke, D. *Inorg. Chem.* **1997**, *36*, 2413−2419.

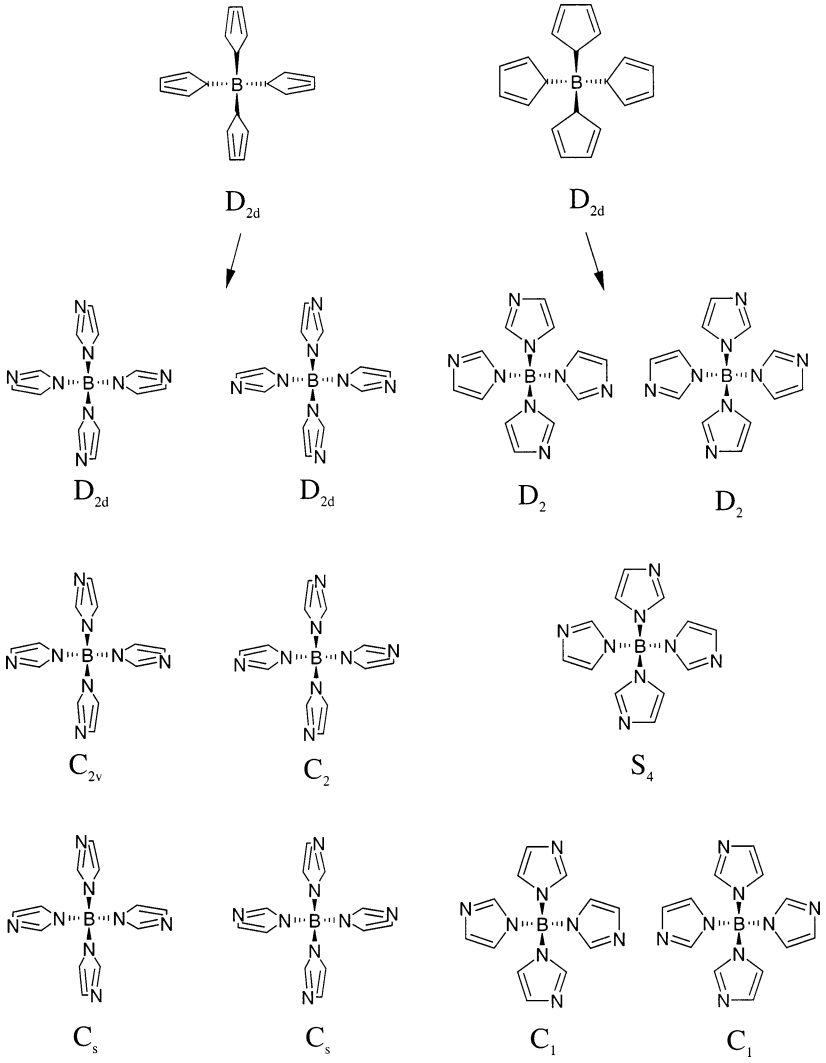

Figure 3. Possible closed (left) and open (right) geometries for $B(Im)_4^-$. In the closed conformations, the ring lies in the plane of the N−B−N bond.

distances in the axial position expand from 2.075(3) to 2.3190(16) and 2.457(4) Å as one goes down the period. The bond lengths in the borates do not change significantly over the three compounds, however, and thus the increase in volume in the unit cell in the almost identical $Ca[B(Im)_4]_2(H_2O)_2$ and $Sr[B(Im)_4]_2(H_2O)_2$ structures is directly attributable to the increase in covalent radius of the metal ion.

Two of the structures ($Ca[B(Im)_4]_2(H_2O)_2$ and $Sr[B(Im)_4]_2(H_2O)_2$) are nearly isomorphous, belong to a triclinic crystal system, and have the $P\bar{1}$ space group. However, the $Mg[B(Im)_4]_2(H_2O)_2$ unit cell is monoclinic and belongs to the $P2_1/c$ space group. The change in symmetry can be explained in part due to two variations in the structure of the Mg compound from that of the Ca and Sr networks. First, the orientations of the imidazole rings bound to the metal in $Mg[B(Im)_4]_2(H_2O)_2$ differ from those found in the Ca or Sr analogues. In the Mg compound, two of the imidazole rings are nearly parallel to the axial ordinate, while the remaining two are almost in the equatorial plane and thus nearly orthogonal to the axial ordinate. In the Ca and Sr compounds, two of the imidazole rings are in the plane of the axial ordinate, but the remaining two imidazole rings significantly deviate from the equatorial position observed in the Mg network solid. In $Ca[B(Im)_4]_2(H_2O)_2$, these two imidazole rings are nearly orthogonal to the equatorial plane, but tilted ∼30° off of the B−N ordinate. In the Sr compound, this same tilt is also observed, but there is an additional ∼45° twist relative to the equatorial plane.

Second, one of the most significant variations between the monoclinic and triclinic forms is the extent of hydrogen bonding in the solid, as shown in Figure 5. In each structure, there are two borates per metal ion for a total of eight imidazole rings. Only four of these imidazoles are coordinated to equatorial positions on the metal center, leaving four additional imidazole rings that are not involved in direct metal−ligand bonding. In the Ca and Sr structures, the noncoordinating rings are engaged in hydrogen bonding to axially coordinated waters, forming two bonds per bound solvent molecule (Ca, 1.90, 1.87 Å; Sr, 1.98, 1.86 Å N−H bond distances). However, in $Mg[B(Im)_4]_2(H_2O)_2$, only one hydrogen bond is observed per water molecule and the noncoordinating imidazole rings (1.61 Å N−H bond distance). The remaining two imidazole rings do not exhibit any significant interactions to either the axial water molecules or the metal centers in $Mg[B(Im)_4]_2(H_2O)_2$. The observed differences in hydrogen bonding can be directly attributed

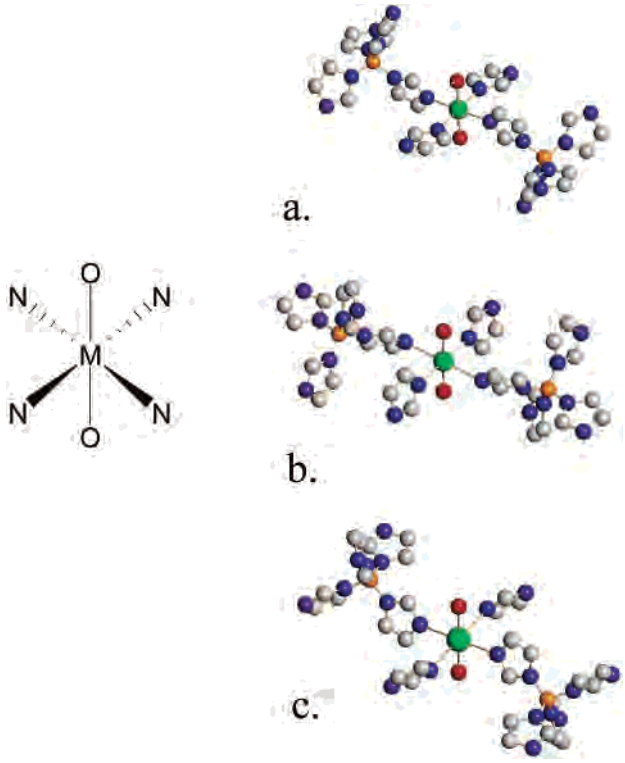

Figure 4. The coordination environments about the metal in $M[(B(Im)_4]_2(H_2O)_2$, where M = Mg (a), Ca (b), and Sr (c).

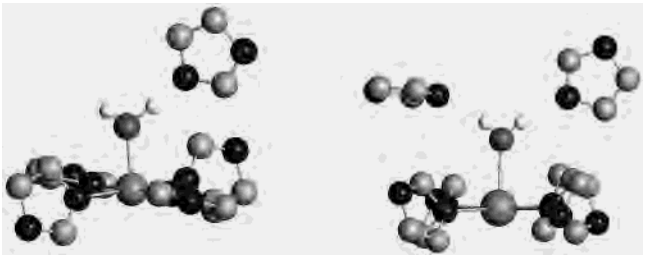

Figure 5. Hydrogen-bonding interactions between imidazole and axially bound water in compound **2** (left) and compound **4** (right). Compound **3** has hydrogen bonding identical to that of **4**.

to the nature of the metal−oxygen bond. The strength and polarity of the Mg−O bond reduces the ability of the bound solvent water molecules to engage in hydrogen bonding with nearby pendant imidazole rings. In the Ca and Sr compounds, this bond is weak enough that the axial water can donate both protons for hydrogen bonding to adjacent imidazole nitrogens.

In the extended network solid of the Mg compound, the metal−borate units form a layered structure (Figure 6). The pattern of these layers resembles an interlaced "brick wall" format. The imidazole−water hydrogen bonds occur within

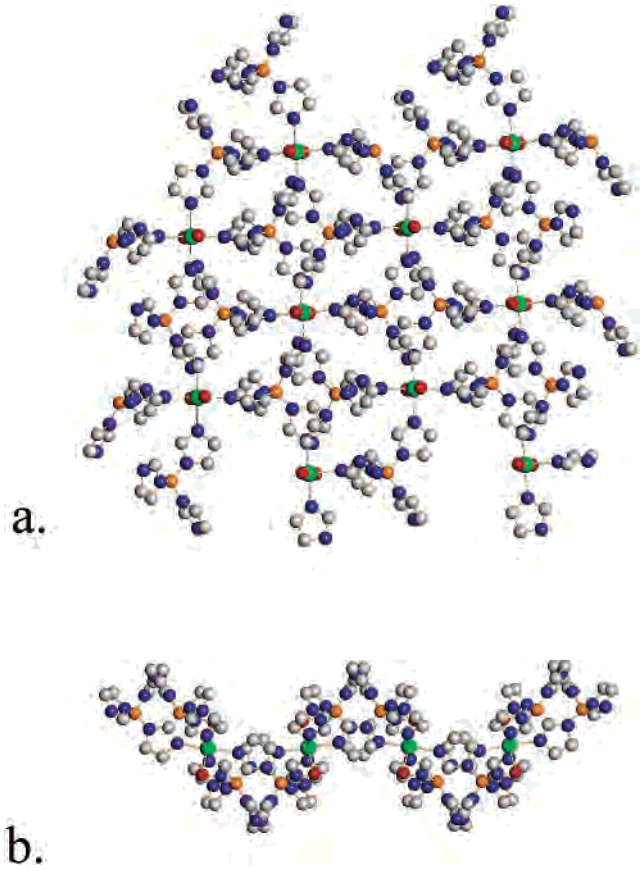

Figure 6. Extended network structure of $Mg[B(Im)_4]_2(H_2O)_2$, along the (a) *a* axis and the (b) *c* axis. The interlaced brick pattern can be seen in view a, while the discrete layering of the structure can be seen in the view along the *c* axis (b). Hydrogen atoms have been omitted for clarity.

the same layer, and the remaining noncoordinating imidazole rings fill the space generated by the slight zigzag motion of the layer itself. In the $Ca[B(Im)_4]_2(H_2O)_2$ and $Sr[B(Im)_4]_2(H_2O)_2$ structures, the metal−borate units form one-dimensional chains in a linked diamond fashion, where two tetrakis(imidazolyl)borate units bridge metal sites (Figure 7). The remaining four imidazole rings of this bridge are engaged in hydrogen bonding to solvent waters on adjacent chains, one to each of the four chains surrounding every one-dimensional coordination assembly.

The formation of interlaced squares in $Mg[B(Im)_4]_2(H_2O)_2$ versus one-dimensional chains in the $Ca[B(Im)_4]_2(H_2O)_2$ and $Sr[B(Im)_4]_2(H_2O)_2$ structures results from how the borates can link together metals in either a one- or two-dimensional network. A diagram displaying how the molecular components of these solids fit together can be found in Figure 8. If a cis pair of borates on a metal is joined to the same adjacent

Table 3. Selected Bond Distances and Angles about the Metal Center for Compounds **2**−**4**

	2	**3**	**4**
		Bond Lengths (Å)	
M−O	2.075(3)	2.3190(16)	2.457(4)
M−N	2.188(3), 2.193(3)	2.4760(19), 2.4904(16)	2.631(4), 2.645(4)
		Bond Angles (deg)	
O−M−O	180.0	180.0	180.0
N−M−O	90.11(14), 89.89(13), 90.62(13), 89.38(13)	92.95(7), 87.05(7), 83.23(6), 96.77(6)	85.29(14), 94.71(14), 99.56(13), 80.44(13)
N−M−N (cis)	89.41(13), 90.59(13)	90.78(5), 89.22(5)	90.95(12), 89.05(12)
N−M−N (trans)	180.0	180.0	180.0

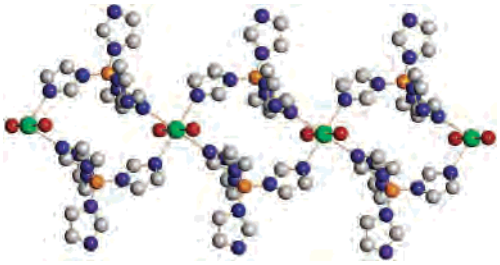

Figure 7. The one-dimensional chains viewed along the *a* axis for Ca-$[B(Im)_4]_2(H_2O)_2$. The strontium structure is isomorphous, and hydrogen atoms have been omitted for clarity.

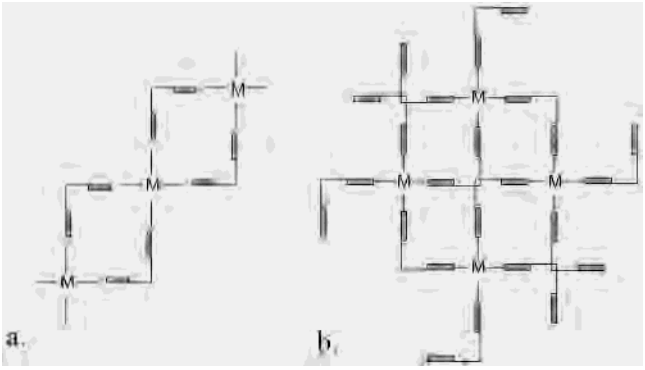

Figure 8. Illustrations of the two types of solid morphologies observed for $M[B(Im)_4]_2(H_2O)_2$.

metal center, then a one-dimensional chain of metal−imidazole squares results. This geometry is shown in Figure 8a and is observed in the Ca and Sr compounds. However, if this same cis pair of borates goes to different metal centers, then alternative geometries could occur depending on whether the resulting network is two- or three-dimensional. In the planar case, this leads to the interlaced block pattern (Figure 8b) observed in the magnesium network solid. The metal−borates close in a figure-8 loop through cis linkages on the metals.

In all of the structures presented in this paper, the borates adopt a chiral conformation although tetrakis(imidazolyl)-borate is not itself a chiral anion. In the protonated form, the enantiomers crystallize out separately into right- and left-handed crystal forms, while in the metal network solids there is an inversion center and thus both enantiomers are observed in the structures. The generation of a chiral solid by using enantiomerically pure conformers of tetrakis(imidazolyl)-borate is unlikely. Although we are still in the process of calculating the energy barriers for isomerization of this anion, previous work on the energies of isomerization of tetraarylmethanes show that rapid equilibration of all isomers occurs at room temperature.[13] In the solution phase, the ^1H NMR spectrum of $B(HIm)(Im)_3$ in CD_3OD does not change over the temperature range of 30 to −60 °C. In order to construct a chiral tetrakis(imidazolyl)borate metal−organic framework, either a substituted tetrakis(imidazolyl)borate that inhibits rotation or a chiral borate (with four different imidazole substitutents around the boron) should be employed.

Changing the metal ion in these solids not only changes the topology of the network but also affects the chemistry exhibited by the network. In the TGA measurements of the three metal−organic frameworks, the axial water molecules can be driven off with increasing temperature. The temperature at which these water molecules are removed decreases as one goes down the period, due to the decreasing strength of the metal−water bond. Since the water molecules at the axial sites of the metals in these coordination polymers can be removed, they can be considered as open metal sites in these solids. We are currently investigating the substitution of coordinated water molecules through incubation of these crystals in other Lewis basic solvents, such as ammonia.

As can be seen in the three metal−organic networks presented in this report, the nature of the metal ion can be used to tune the structure of the solid. In the cases presented here, a combination of the radius of the metal and its electronic character affect the topology of the resultant solid. Several parameters change as one goes down the period, including the closed/open conformation of the borate, the geometry of the imidazoles about the metal center, and the lengths of the metal−ligand bonds. These variations in geometries and hydrogen bonding result in differences between the magnesium structure, which adopts a brick wall layered pattern, and the calcium and strontium structures, which form one-dimensional square chains. We are continuing our work on these solids, including modifying the borate structure and examining the exchange of the axial water molecules.

Acknowledgment. C.J.Z. acknowledges the University of Akron for a faculty research grant (FRG-1524). We also wish to acknowledge NSF Grant CHE-0116041 for funds used to purchase the Bruker-Nonius diffractometer and the Kresge Foundation and donors to the Kresge Challenge Program at The University of Akron for funds used to purchase the NMR instrument used in this work.

Supporting Information Available: Thermogravimetric analyses and crystallographic information files (cif). This material is available free of charge via the Internet at http://pubs.acs.org.

IC026244X